Volume Title: Risks in Agricultural Supply Chains

Volume Authors/Editors: Pol Antràs and David Zilberman, editors

Volume Publisher: University of Chicago Press

Volume ISBNs: 978-0-226-82922-7 (cloth)

Volume URL: https://www.nber.org/books-and-chapters/risks-agricultural-supply-chains

Conference Date: May 20-21, 2021

Publication Date: August 2023

Chapter Title: Fertilizer and Algal Blooms: A Satellite Approach to Assessing Water Quality

Chapter Author(s): Charles A. Taylor, Geoffrey Heal

Chapter URL: https://www.nber.org/books-and-chapters/risks-agricultural-supply-chains/fertilizer-and-algal-blooms-satellite-approach-assessing-water-quality

Chapter pages in book: p. 83 – 105

4

Fertilizer and Algal Blooms
A Satellite Approach to Assessing Water Quality

Charles A. Taylor and Geoffrey Heal

4.1 Introduction

The US Environmental Protection Agency considers nutrient pollution one of the "most widespread, costly and challenging environmental problems."[1] Increasing flows of nitrogen have far exceeded the Earth's carrying capacity and have impaired ecosystem functioning (Vitousek et al. 1997; Gruber and Galloway 2008; Erisman et al. 2013), and nutrient levels far exceed the planetary boundaries of certainty (Steffen et al. 2015).

Nutrient enrichment, hypoxia, and algal blooms are interrelated environmental phenomena. They are caused by excess nitrogen and phosphorus, coming primarily from fertilizer use but also from human and industrial waste. These nutrients leach into waterways and feed the growth of phytoplankton in a process called eutrophication (Nixon 1995). Eutrophication can produce algal blooms, which are considered harmful when concentrations of algae (e.g., cyanobacteria) achieve sufficient density to create negative environmental or health effects (Smayda 1997).

Occurring in both fresh and salt water, algal blooms can be produced by excess nutrients and climactic anomalies like warmer water tempera-

Charles A. Taylor was working toward his PhD in Sustainable Development at Columbia University when this chapter was written, and is currently an S.V. Ciriacy-Wantrup postdoctoral fellow at the University of California, Berkeley.

Geoffrey Heal is a professor of economics at Columbia Business School and a research associate of the National Bureau of Economic Research.

Taylor received support from the Center for Environmental Economics and Policy (CEEP), Columbia University. For acknowledgments, sources of research support, and disclosure of the authors' material financial relationships, if any, please see https://www.nber.org/books-and-chapters/risks-agricultural-supply-chains/fertilizer-and-algal-blooms-satellite-approach-assessing-water-quality.

1. Source: www.epa.gov/nutrientpollution/issue, accessed December 9, 2020.

tures (Paerl and Huisman 2008; Michalak et al. 2013; Ho, Michalak, and Pahlevan 2019). Algal blooms are often followed by hypoxic aquatic conditions, defined by dissolved oxygen levels below two ml per liter, as dead phytoplankton sink to the seafloor and are decomposed by bacteria. Sustained low oxygen levels, in turn, can result in aquatic dead zones.

Algal blooms have increased in frequency and intensity over the decades (Anderson 1989; Hallegraeff 1993; Hudnell 2008; Huisman et al. 2018; Ho, Michalak, and Pahlevan 2019). The quantity and extent of dead zones have also increased across the globe (Diaz and Rosenberg 2008). Dead zones are now considered a major threat to the health of aquatic ecosystems (Diaz and Rosenberg 2008; Doney 2010). While natural processes like upwelling of nutrient-rich ocean water contribute to eutrophication, anthropogenic nutrient loading is increasingly the driver of algal blooms and hypoxic events.

Fertilizer use is mostly exempt from federal regulation under the Clean Water Act despite being the major source of water quality impairment in the US (Olmstead 2010), and individual states have been hesitant to regulate agricultural inputs (Kling 2013). While regulation of agriculture is politically difficult to implement, several other challenges also inhibit efficient regulation of this market.

First, the economic impacts of hypoxia and algal blooms and the related external cost of fertilizer are difficult to quantify (Rabotyagov et al. 2014; Barbier 2012). This is partly due to the inherent challenges of estimating the costs of nonpoint pollution (Shortle and Horan 2001, 2013), in which it is difficult to link accumulated downstream pollution to specific upstream sources. In an analysis of contributors to the dead zone in the Gulf of Mexico, David, Drinkwater, and McIsaac (2010) found that the highest nitrogen yields occurred in the tile-drained Corn Belt of Minnesota, Iowa, Illinois, Indiana, and Ohio—areas 1,500 km upstream from the pollution culmination point at the mouth of the Mississippi River.

A second challenge to rigorous estimation of the social cost of fertilizer is the lack of temporally consistent and spatially relevant data on water quality (Brooks et al. 2016) that can be linked to economic outcomes. Water quality studies rely on data from *in situ* samples of water bodies, which are limited in temporal and spatial extent and face challenges related to inconsistent sampling practices and lack of coordination between scientific and governmental entities (Monitoring Water Quality 1995).[2] Past studies of the impact of algal blooms have been limited to specific geographies or relatively short time frames. To overcome this problem, we construct a measure of county-level algal bloom intensity that is derived from over three decades of Landsat satellite imagery, as well as a spatially weighted measure of fertilizer use that is linked to watersheds.

2. The availability of standardized historic water quality data has improved following the launch of the Water Quality Portal by USGS, EPA, among others (Read et al. 2017).

4.2 Data

Algal blooms: We construct a county-level measure of algal bloom intensity derived from over three decades of Landsat satellite imagery and processed using computing power available through Google Earth Engine.[3] Several satellite products have been used to detect and monitor algal blooms, including the European Space Agency's Medium Resolution Imaging Spectrometer (MERIS) product (Clark et al. 2017) and a Moderate Resolution Imaging Spectroradiometer (MODIS) product for ocean color, which measures chlorophyll levels at 500 m resolution in the ocean and large inland lakes. Each satellite product has its own trade-offs around duration, revisit time, resolution, and geographic extent. We opt for Landsat given its longer time series and the higher spatial resolution at 30 m, which allows us to better capture small inland water bodies and rivers.

We build on the approach of Ho, Michalak, and Pahlevan (2019) to analyzing global lakes. We use Landsat Thematic Mapper top-of-atmosphere (TOA), combining Landsat 5 (1984–2000) and Landsat 7 (2000–present). The bloom algorithm is based on the near-infrared (NIR) band with an atmospheric correction for shortwave radiation (SWIR): B4 − 1.03*B5 (Wang and Shi 2007). In matching Landsat 5 with Landsat 7, we subtract the satellite bias based on the difference in county-level bloom values during the years in which the products overlapped.

We filter out all images with over 25 percent cloud cover. Unlike Ho et al. (2017), we do not filter out pixels beyond a certain hue threshold. We then take the temporal average of the bloom measure across all the 16-day revisit periods for each pixel during the peak bloom time in late summer (July to September). Next, we take the US county-level mean over a 30 m water mask from the National Land Cover Dataset (NLCD) for the maximum water extent from 2001 to 2016. US state boundaries extend three nautical miles from the coast, and this area is included in each state's county calculations of bloom intensity. We thus include both saline coastal waters and inland fresh water. We exclude counties lacking significant water features (less than 5 km^2 of surface water), dropping about 25 percent of US counties. However, the results are robust to their inclusion.

It is worth noting that our calculated index is not a direct measure of concentrations of either chlorophyll or any specific algal species; rather, it measures relative greenness in the upper layer of the water column. Many studies over the years have used Landsat to identify algal blooms (Tyler et al. 2006; Duan et al. 2007; Tebbs, Remedios, and Harper 2013). This specific algorithm has been validated on the ground in Lake Erie (Ho et al. 2017) and globally through tests of how the index reflects the spatial gradients of chlorophyll-a levels within lakes (Ho, Michalak, and Pahlevan 2019).

3. Google Earth Engine, https://earthengine.google.com.

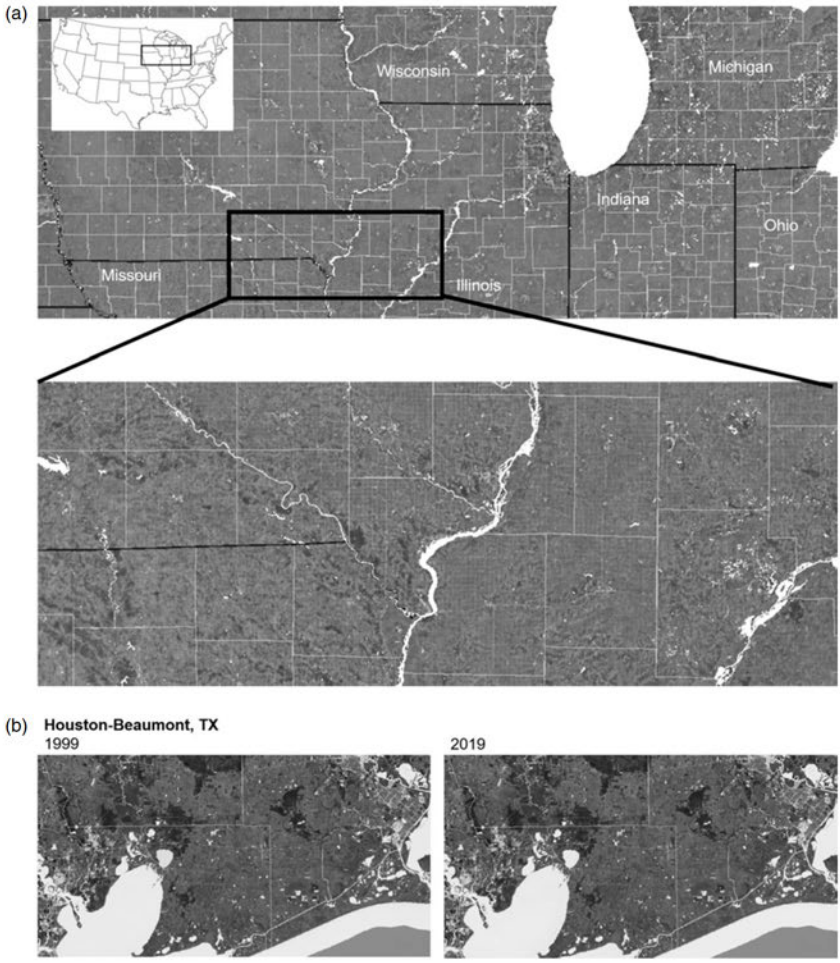

Figure 4.1 Panel A shows late summer bloom index averaged over 20 years from 1999 to 2019 in the US Corn Belt, then with a close-up of the boundary region of Iowa, Illinois and Missouri, where the Des Moines River meets the Mississippi. Panel B shows the late summer algal bloom index at two discrete points in time (1999 and 2019) in the Houston-Beaumont region.

The construction of our bloom index can be visualized in panel A of figure 4.1, along with how the bloom index changes over time in panel B.

Fertilizer: We employ the US Geological Survey (USGS)'s annual county-level estimates of nitrogen and phosphorus use from 1987 to 2012 (Brakebill and Gronberg 2017), which was recently updated for the year 2017 (Falcone 2021). Data are based on fertilizer product sales compiled by the Association of American Plant Food Control Officials (AAPFCO), and thus exclude organic fertilizers like manure. We normalize fertilizer values by the

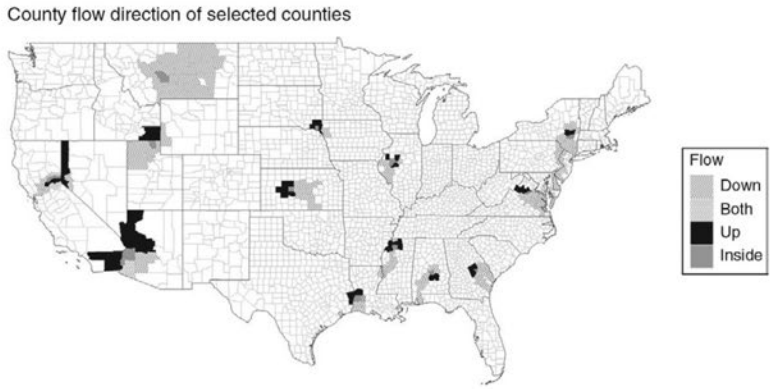

Figure 4.2 Watershed classification of counties based on their relative location within the USGS NHD hydrologic unit code HUC 4 watershed boundary. Thirteen randomly selected counties are shown in gray. Areas with diagonal lines represent counties that are at least partly within the same HUC 4 and downstream from the gray county, as determined by their overlap with finer resolution HUC 12 watersheds. Likewise, black counties are upstream from gray counties. Finally, the areas with dashed lines, "Both," include counties that have land area that is both upstream and downstream from gray counties.

land area in a given county. We further calculate the sum of fertilizer use in upstream counties within a given watershed (HUC 4) from a county. The upstream-downstream relationship for a random subset of counties can be visualized in figure 4.2. Our main measure is farm fertilizer use, but results hold including non-farm fertilizer use as well.

The upstream-downstream analysis is based on USGS watershed boundaries of hydrologic unit code HUC 4 and HUC 12 to assign water flow relationships between counties using flow relationships from the National Hydrography Dataset (NHD) (Buto and Anderson 2020).

County-level climate data come from NOAA's Climate Divisional Database (nCLIMDIV) of monthly temperature and precipitation levels. Annual estimates of hypoxic extent in the northern Gulf of Mexico spanning 1985 to 2019 come from Nancy Rabalais, LUMCON, and R. Eugene Turner, LSU.[4] County-level data on agricultural yields come from the US Department of Agriculture's historical census and National Agricultural Statistics Service (NASS).

4.2.1 Validation of Satellite Algal Bloom Measure

To provide evidence that our algal bloom measure is both accurate and representative nationally, we compare our Landsat algal measure to a recent

4. Source: https://www.epa.gov/ms-htf/northern-gulf-mexico-hypoxic-zone.

Table 4.1 **Relationship between measures of Landsat algal bloom and Sentinel-3 chlorophyll**

	Dependent variable: Sentinel-3 Chlorophyll			
	(1)	(2)	(3)	(4)
Landsat bloom	195.47***	146.44***	151.57***	100.24***
	(30.90)	(23.99)	(18.38)	(31.51)
Climate controls		X	X	X
Spatial FE			Division	County
Observations	9,109	9,109	9,109	9,109
R^2	0.19	0.23	0.34	0.64

Note: Linear regression. Dependent variable is Sentinel-3 OLCI band 11 (Chl fluorescence baseline, red edge transition). Predictor is Landsat algal bloom intensity measure used in this paper. Both measures aggregated at county-level from July to September over areas with water. Time series from 2017 to 2020 when both satellite products available. Counties with less than 5 km^2 of water dropped from analysis. Standard errors clustered at the state level. * $p < 0.1$; ** $p < 0.05$; *** $p < 0.01$

satellite product for chlorophyll-a, an indicator of algal activity. We make the comparison at the county-year level, using a similar construction by averaging values over water area in a county and across July to September. Since late 2016, the Sentinel-3 Ocean and Land Color Instrument has provided chlorophyll measures at 300 m resolution with a two-day revisit time. We use the band at 709.75 nm for chlorophyll fluorescence baseline, red edge transition. While MODIS has an Ocean Colour SMI Chlorophyll-a product going back to 2000, we do not use this measure due to its even lower resolution and geographic restriction to primarily oceanic and coastal regions. Table 4.1 shows the results of regressing Sentinel chlorophyll on our Landsat algal bloom measure at the county-year level. We find a strong positive relationship as expected, which persists with controlling for climate and various spatial fixed effects.

Figure 4A.1 shows a scatterplot of these two measures of water quality at the county-year level from 2017 to 2020, splitting counties into quartile by water area. We note a positive relationship, which improves with amount of water in an area. The weak relationship in the first quartile motivates the fact that we drop counties in the first quartile (less than 5 km^2 water area) from our general analyses. Figure 4A.2 shows a similar scatterplot but facets across regions to test the generalizabilty across the US. We find a generally positive relationship between our Landsat measure of bloom intensity and Sentinel chlorophyll at the county-year level in all places except the Mountain region. It is worth noting that this region is the driest part of the US with the lowest proportions of water area by counties.

Altogether, we take the persistent correlation we see between our Landsat algal bloom measure and Sentinel chlorophyll at the county level to mean

Table 4.2 **Bloom algorithm and *in situ* measurements of chlorophyll-a**

	Dependent variable: Chlorophyll-a concentration (ug/L)						
	(1)	(2)	(3)	(4)	(5)	(6)	(7)
Bloom	0.066***	0.063***					
	(0.010)	(0.008)					
Bloom:Estuary			0.031***	0.031***	0.024***	0.024***	0.027***
			(0.010)	(0.009)	(0.007)	(0.007)	(0.005)
Bloom:Lake			0.065***	0.072***	0.065***	0.064***	0.039***
			(0.008)	(0.009)	(0.008)	(0.009)	(0.008)
Bloom:Stream			0.042***	0.044***	0.043***	0.044***	0.024***
			(0.011)	(0.010)	(0.008)	(0.007)	(0.005)
RGB controls	No	Yes	Yes	Yes	Yes	Yes	Yes
Month FE	No	No	No	Yes	Yes	Yes	Yes
Geo FE	No	No	No	No	Grid	County	Site
Observations	137,246	137,246	137,246	137,246	137,246	137,246	137,246
R^2	0.070	0.165	0.171	0.182	0.305	0.355	0.629

Note: Linear regression. Dependent variable is *in situ* chlorophyll-a concentration from on-the-ground sampling. Bloom is the computed Landsat algal bloom measure. Observations filtered to exclude images with less than 50 percent water in surrounding pixels and more than 25 percent cloud cover. Outliers beyond the 99.9th percentile dropped. RGB includes controls for Landsat's red, green, and blue radiance bands. Standard errors clustered at the HUC 4 watershed level. * $p < 0.1$; ** $p < 0.05$; *** $p < 0.01$.

that both are measuring broadly similar phenomena. A perfect correlation would not be expected, given that these two measures aggregate millions of images over an entire county's water area from independent satellite products with different spatial resolutions and revisit times to create one annual value per county.

For further validation, we compare our Landsat measure of algal bloom intensity to *in situ* measurements of chlorophyll at the individual site level—instead of aggregating over time and space. To do so, we employ the Aquasat data set, which matches over 600,000 *in situ* water quality measures (including total suspended sediment, dissolved organic carbon, chlorophyll-a, and Secchi disk depth) with spectral reflectance from Landsat 5, 7, and 8 collected within one day of the sample over 1984 to 2019 (Ross et al. 2019). We calculate an image-specific algal bloom measure using the same algorithm used in our paper (Wang and Shi 2007).

Results are shown in table 4.2. At the site level, we see a consistently positive relationship between sampled chlorophyll-a concentration and our site-specific Landsat algal bloom measure, holding across the three main water type classifications in the Aquasat data set (estuary, lake, and stream).

4.2.2 Satellite-Derived Bloom Intensity Trends

Figure 4.3 showcases the temporal and spatial patterns of the constructed bloom index across US counties. As expected, bloom intensity is higher

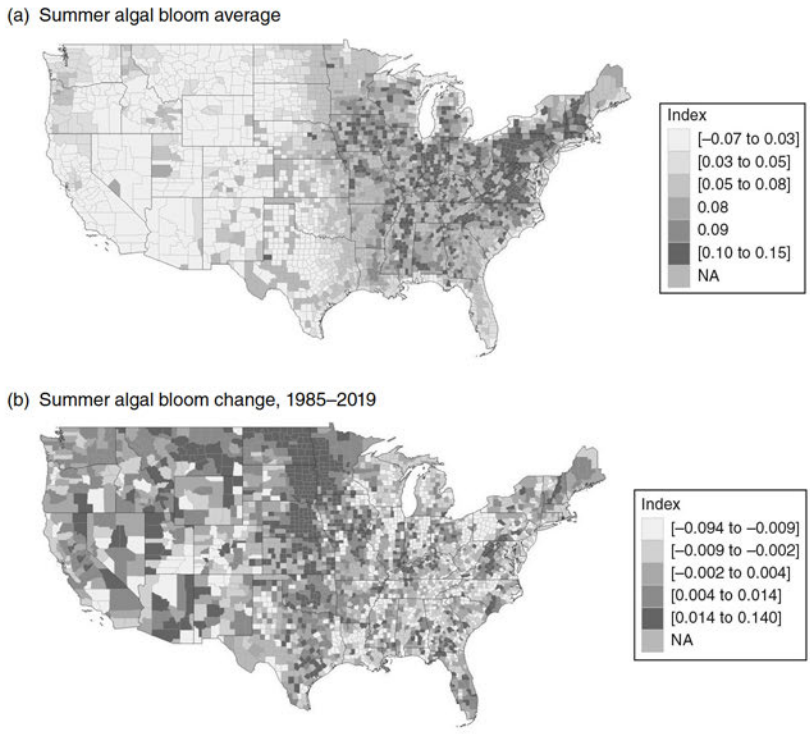

Figure 4.3 Panel A plots the county-level late summer bloom index averaged over the entire sample time period from 1984 to 2020. Panel B plots long-term change from 1985 to 2019 using three-year averages around the endpoints (i.e., 1984–1986 for 1985). Gray counties lack enough surface water for a reading.

in agricultural regions. There is significant geographic variation in where bloom intensity increased and decreased, although there seems to be a general upward trend in the upper Great Plains and along the 100th meridian.

Figure 4.4 graphs average annual bloom intensity by US region from 1984 to 2020. Trends appear flat or decreasing in most locations. Decreasing bloom intensity in the US Southeast (South Atlantic) signifying potential water quality improvement may be attributable to a reduction in cropland area in that region. Algal blooms have intensified in the upper Midwest (West North Central) beginning in the mid-2000s. This may be linked to Corn Belt cropland expansion and intensification driven by ethanol demand in response to the Energy Policy Act of 2005, as noted by others (Metaxoglou and Smith 2021). We see that four of the five largest ethanol producers in the US are included in the West North Central division (Iowa, Nebraska, South Dakota, Minnesota).

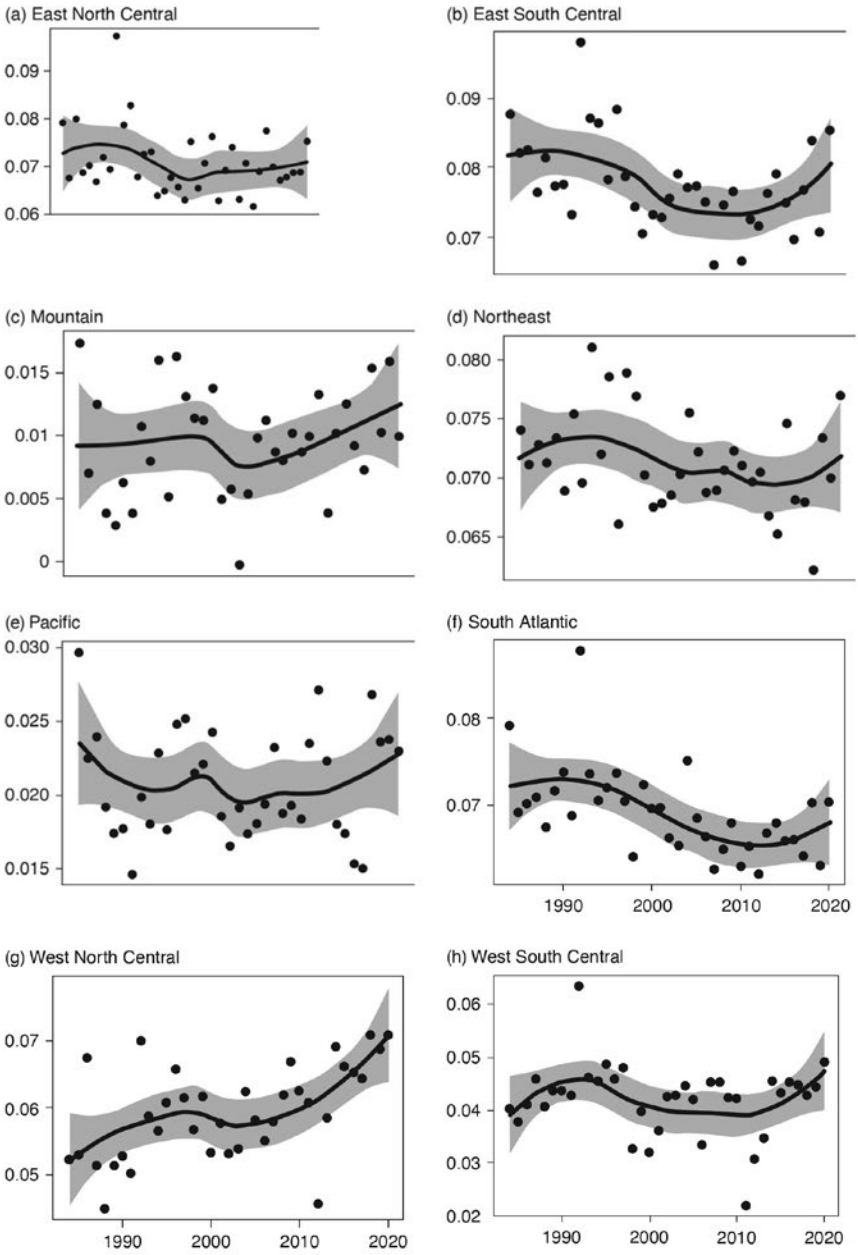

Figure 4.4 Trends in late summer algal bloom intensity from 1984 to 2020 by US Census division. "Northeast" includes New England and the Middle Atlantic. Legend map in panel (i) below.

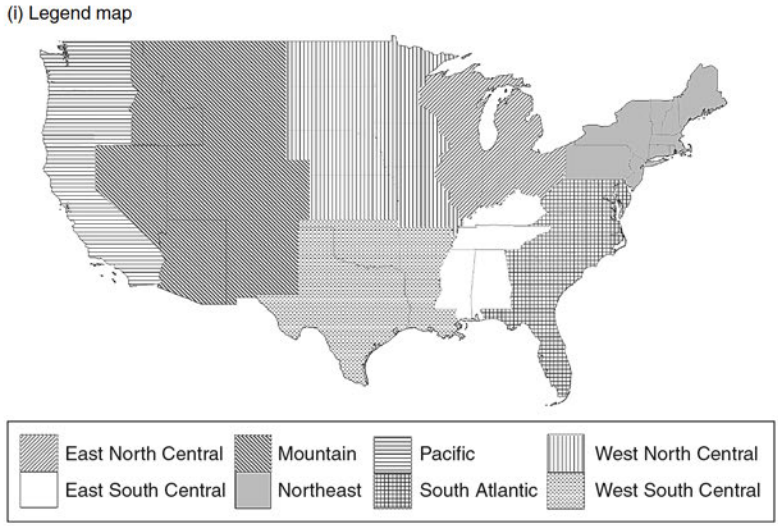

Figure 4.4 (continued)

Notwithstanding some anomalies in recent years, the overall improvement in water quality that we see aligns with Topp et al. (2021), who use a similar approach to ours that links Landsat to *in situ* measures of water quality to model water clarity over 14,000 lakes in the US. They find a marked improvement in water quality over time. Our findings also align with Keiser and Shapiro (2019), who note a reduction in water pollution through 2001 using *in situ* data.

4.3 Empirical Strategy

We employ several empirical approaches: a panel approach of county-year observations to assess annual variation; a five-year panel to assess intermediate variation; and a long-difference cross-sectional approach to assess longer-term effects. We apply these approaches to estimate the impact of fertilizer on algal blooms.

Panel

$$bloom_{it} = \beta_1 fert_{itw} + \beta_2 W_{it} + state_{s(i)} + \alpha_i + \gamma_t + \varepsilon_{it}. \quad (1)$$

Long-difference

$$\Delta bloom_i = \beta_1 \Delta fert_i + \beta_2 \Delta W_i + state_{s(i)} + \varepsilon_i. \quad (2)$$

In the panel model, the outcome variable, *bloom*, is the satellite-derived measure of late summer algal bloom intensity in county i and year t. *fert* is tons of nitrogen fertilizer in county i and year t, or alternatively the sum of fertilizer use in counties upstream of county i but within its watershed w. Fertilizer values are normalized by dividing by county land area. W is a vector of climate controls including mean summer *temp* and *precip*.

County-level fixed effects α are used to demean the observations and allow for interannual comparisons, as well as year-level fixed effects γ to account for national-level variation (i.e., commodity prices). State-specific annual time trends *state* are also included to account for differential state-level policy. Standard errors are clustered at the state level s.

In the long-difference, the outcome variable, $\Delta bloom$, is the change in our satellite-derived measure of late summer algal bloom intensity between 1987 and 2017, each period calculated as a three-year average (i.e., period 1987 is the average of 1986 to 1988) to reduce the likelihood of anomalous years influencing outcomes. Similarly, $\Delta fert$ and ΔW represent the change in each variable at the county level over that same time period. We also employ state-level fixed effects, *state*, to isolate within-state variation. Standard errors are again clustered at the state level. Note we restrict our analysis to the continental US. To ensure a clear satellite signal for water quality, we drop counties with less than 5 km^2 of water cover (one-quarter of US counties), as well as counties with no cropland. However, results are robust to the inclusion of such counties.

For robustness, we also estimate "intermediate" effects with a panel of five-year intervals using three-year rolling-window moving averages calculated over our annual panel data set. This allows us to account for a multi-year process. For example, it can take several years for fertilizer to leach into downstream waterways (Rabotyagov et al. 2014), and likewise, fertilizer use over a multi-year period may result in elevated bloom intensity over the course of several years. For this intermediate analysis, we utilize the five-year panel of county-level fertilizer data developed by Falcone (2021).

4.4 Results

4.4.1 Drivers of Fertilizer Use

Nitrogen fertilizer consumption in 2015 in the US was 13 million tons,[5] and world nitrogen demand was 119 million tons in 2019 (FAO 2018). Nitrogen usage has steadily increased over the last couple of decades, aided by the Haber-Bosch process and low-cost energy (Glibert 2020), while the use of phosphate and potash-based fertilizers has flattened or declined, as shown

5. Fertilizer Use and Price: www.ers.usda.gov/data-products/fertilizer-use-and-price.

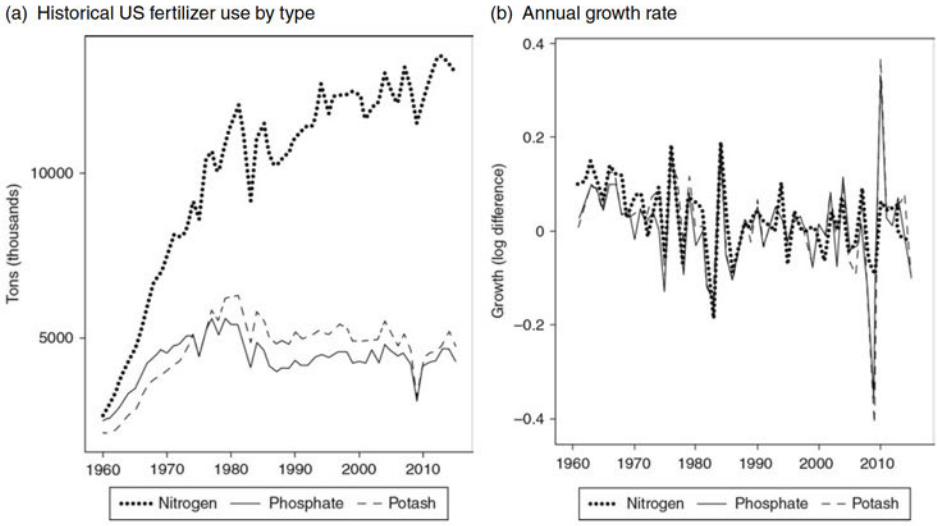

Figure 4.5 USDA ERS fertilizer use aggregated nationally by fertilizer type and year

in figure 4.5. However, phosphates are also an important driver of algal blooms. Figure 4A.3 plots the relationship between nitrogen and phosphate use at the county level. Again, we see a very high correlation.

We first analyze the drivers of fertilizer use at the county level. For an individual farmer, the yield-response curve for fertilizer use is well-known. As described earlier, nitrogen fertilizer accounts for a large cost component of commercial farm operations (~10 percent of production value). There is a strong incentive to apply an amount that optimizes yield response relative to the marginal cost of fertilizer. Since fertilizer and crops have transparent commodity pricing, we are not concerned about pricing differentials across location driving changes in input use.

At the county level we expect fertilizer use to be driven by changes in land use. In table 4.3, we regress county-level nitrogen use on several potential land use variables: total harvested acres of the four major crops in the US (corn, soy, wheat, cotton), the ratio of corn-to-soy acres, and acres of land enrolled under the USDA Conservation Reserve Program (CRP). Cropland area is strongly related to nitrogen use. We would expect that places that increased corn production relative to soy production would increase their nitrogen fertilizer use given that soybeans are nitrogen-fixing leguminous plants that require less nitrogen compared to corn. Finally, we see a negative relationship with CRP enrollment, which makes sense given that this program entails taking land out of active farm production.

Overall, these results reassure us that fertilizer use is responding to the

Table 4.3 **Drivers of farm nitrogen use**

	Dependent variable: Nitrogen use (1,000 tons)			
	(1)	(2)	(3)	(4)
Crop area	0.009***	0.012***	0.009***	0.012***
	(0.003)	(0.003)	(0.003)	(0.003)
Corn-soy ratio		0.929***		0.920***
		(0.252)		(0.248)
CRP acres			−0.008***	−0.010**
			(0.003)	(0.004)
County FE	X	X	X	X
Year FE	X	X	X	X
State-Yr trends	X	X	X	X
Observations	83,094	51,538	82,804	51,458
R^2	0.954	0.956	0.954	0.956

Note: Linear regression. Dependent variable is aggregate farm-level nitrogen use (1,000s of tons) at the county level. Crop area is the total harvested acres of corn, soy, wheat, and cotton. Corn-soy ratio is the amount of corn acres divided by the sum of corn and soybean acres. CRP acres is the amount of acres under the USDA Conservation Reserve Program. Time series to 1987 to 2012 and 2017. Sample size varies based on extent of counties with both corn and soy production and CRP data. Standard errors clustered at the state level. * $p < 0.1$; ** $p < 0.05$; *** $p < 0.01$.

individual and aggregate-level factors that one would expect and that our nitrogen use data are capturing meaningful variation across counties and over time.

4.4.2 Fertilizer on Blooms

We next test the relationship between nitrogen use and algal bloom intensity at the county level, as captured by a satellite measure of late summer water greenness. In table 4.4 we separately test for the effects of nitrogen use in the county and the sum of nitrogen use over upstream counties within the county's watershed. We further control for weather conditions and county and year fixed effects, as well as state-year trends, as described earlier.

Figure 4.6 plots the coefficients for the annual panel, the five-year panel, and the long difference cross-section over thirty years from 1987 to 2017. We see that algal bloom intensity responds to nitrogen use across short-term, medium-term, and long-term horizons.

There are valid concerns about the extent to which weather is a potential confounder given its influence on farm-level decisions (e.g., reducing fertilizer use in response to adverse weather) as well as bloom intensity directly through phytoplankton biological processes. While we cannot completely untangle this relationship, in figure 4A.4 we run the analyses from figure 4.6 but omit the controls for growing season precipitation and temperature. The resulting coefficients are quite similar.

Table 4.4 **Late summer algal bloom intensity and fertilizer use per km²**

	Dependent variable: Algal boom intensity			
	(1)	(2)	(3)	(4)
Nitrogen, in county	1.409***	0.589*		
	(0.440)	(0.320)		
Nitrogen, upstream			1.576***	0.529
			(0.448)	(0.471)
County FE	X	X	X	X
Year FE	X	X	X	X
State-Yr trend		X		X
Controls	Weather	Weather	Weather	Weather
SE cluster	State	State	State	State
Observations	61,020	61,020	54,221	54,221
R^2	0.856	0.858	0.858	0.860

Note: Linear regression. Dependent variable is county-level average bloom intensity from July to September in areas with water. Nitrogen is 1,000s of tons of farm-level use per km² land area of either county or counties upstream within the HUC 4 watershed. Time series to 1987 to 2012 and 2017. Counties with less than 5 km² of water dropped from analysis. Standard errors clustered at the state level. * $p < 0.1$; ** $p < 0.05$; *** $p < 0.01$.

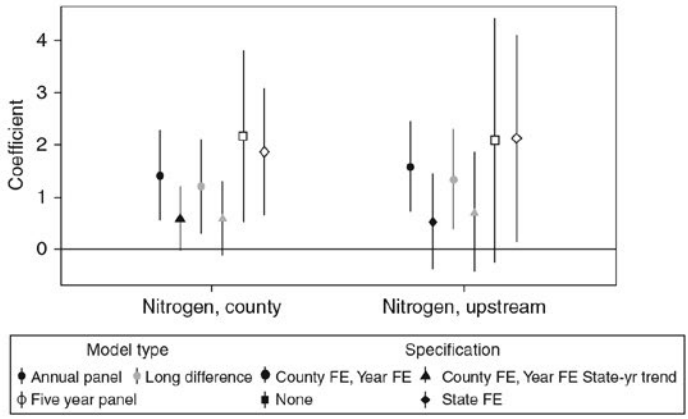

Figure 4.6 **Effect of nitrogen use on late summer algal bloom intensity. Coefficient plot. Lines with black shapes include the same specification as table 4.4. Lines with gray shapes include observations every five years from 1987 to 2017, using average values in the year prior through the year after each point. Lines with white shapes are the results of the cross-sectional long difference from 1987 to 2017, similarly using three-year average values around the endpoints. All models control for average weather conditions. Counties with less than 5 km² of water dropped from analysis. Standard errors clustered at the state level. Error bars are at the 95 percent confidence range.**

Table 4.5 **Mississippi River basin annual nitrogen use and Gulf hypoxia extent**

	Dependent variable:					
	Hypoxia (sq km)			Log Hypoxia (sq km)		
	(1)	(2)	(3)	(4)	(5)	(6)
Nitrogen	4.386**	3.702*	4.633*			
	(2.087)	(1.960)	(2.409)			
Log Nitrogen				6.571**	5.448**	5.709*
				(2.902)	(2.577)	(3.241)
Weather upstream		X	X		X	X
Weather coastal			X			X
Observations	26	26	26	26	26	26
R^2	0.155	0.375	0.398	0.176	0.455	0.456
Adjusted R^2	0.120	0.290	0.247	0.142	0.380	0.320
F Statistic	4.417**	4.407**	2.641*	5.128**	6.117***	3.356**

Note: Linear regression. Dependent variable is Gulf of Mexico summer hypoxic extent as defined by the estimated area where bottom-water dissolved oxygen is below 2 mg/L. Nitrogen is measured in 1,000s of tons for farm use, inverse weighted by distance from the mouth of the Mississippi River and summed across all counties in the Mississippi River basin. Weather controls include average temperature and precipitation from January to June of the given year for all counties in the Mississippi River basin (upstream) and counties along the coast of the Gulf of Mexico (coastal). Time period from 1985 to 2019. * $p < 0.1$; ** $p < 0.05$; *** $p < 0.01$.

4.5 Gulf of Mexico Effect

This paper has focused on the within-county impact of fertilizer on algal blooms in that same county. While we account for nutrient pollution from the fertilizer deployed upstream from the county, we do not explicitly assess downstream impacts. A proportion of all fertilizer applied across the entire Mississippi River basin (3.2 million km^2, or about 40 percent of the continental US including the entire Midwestern Corn Belt) reaches the Gulf of Mexico via the Mississippi River (and the nearby Atchafalaya River). This upstream nutrient pollution creates hypoxic conditions in the Gulf of Mexico (Rabotyagov et al. 2014). Figure 4A.5 shows the correlation between upstream nitrogen and phosphate use and the size of the Gulf of Mexico hypoxic zone. We see the strong correlation between nitrogen and phosphate fertilizer use, as well as a positive but weaker correlation with hypoxic zone extent.

In table 4.5 we estimate the impact of upstream nutrients on the extent of the hypoxic zone. We take the inverse distance-weighted average of fertilizer use across all counties in the Mississippi River basin. Since weather also affects hypoxia via its impact on water flow and phytoplankton activity, we flexibly control for precipitation and temperature across the Mississippi River basin and along the coast. We find a somewhat weak but persistently positive relationship between nitrogen use and hypoxic extent: a 1,000 ton

increase in upstream nitrogen adds 4 km^2 to the hypoxic zone in the Gulf. The average hypoxic zone during this time period was 14,000 km^2. In log form, we see that a 1 percent increase in nitrogen is associated with about a 6 percent increase in hypoxic extent in km^2. We also show the results for phosphates, another important limiting factor in phytoplankton growth (Turner and Rabalais 2013), in table 4A.1.

4.6 Discussion

Estimating the economic cost of fertilizer via water quality is difficult due to the fact that farm pollution is largely exempt under the Clean Water Act, as well as the lack of annual panel on water quality linked to an administrative level. To this end, we create such a data set using a satellite algorithm to approximate algal bloom intensity at the US county level from 1984 to 2020.

We find that fertilizer is a major driver of water quality impairment at an annual and longer-term timescale. Impacts are apparent both locally and downstream from the fertilizer use, extending to the Gulf of Mexico.

We find significant geographic variation in where blooms occur, and where bloom intensity has increased and decreased over time. On average bloom levels have been relatively flat with the exception of an upward trend in the upper Great Plains and along the 100th meridian starting in the mid-2000s. This finding may be linked to Corn Belt cropland expansion and intensification driven by ethanol demand in response to the Energy Policy Act of 2005.

We hope that this new satellite product of water quality can be tested, refined, and utilized in research on other policy-relevant questions, including the valuation of wetlands and other ecosystem services—and assessing the benefits of land use programs such as the USDA's Conservation Reserve Program and Wetlands Reserve Program. For example, wetland protection and restoration may significantly reduce downstream nutrient pollution (Mitsch et al. 2005) while providing co-benefits like flood mitigation (Taylor and Druckenmiller 2021).

Further, given the global nature of remote sensing data, we hope this product can be utilized in an international context where water quality impairment and algal blooms are increasing challenges.

Appendix

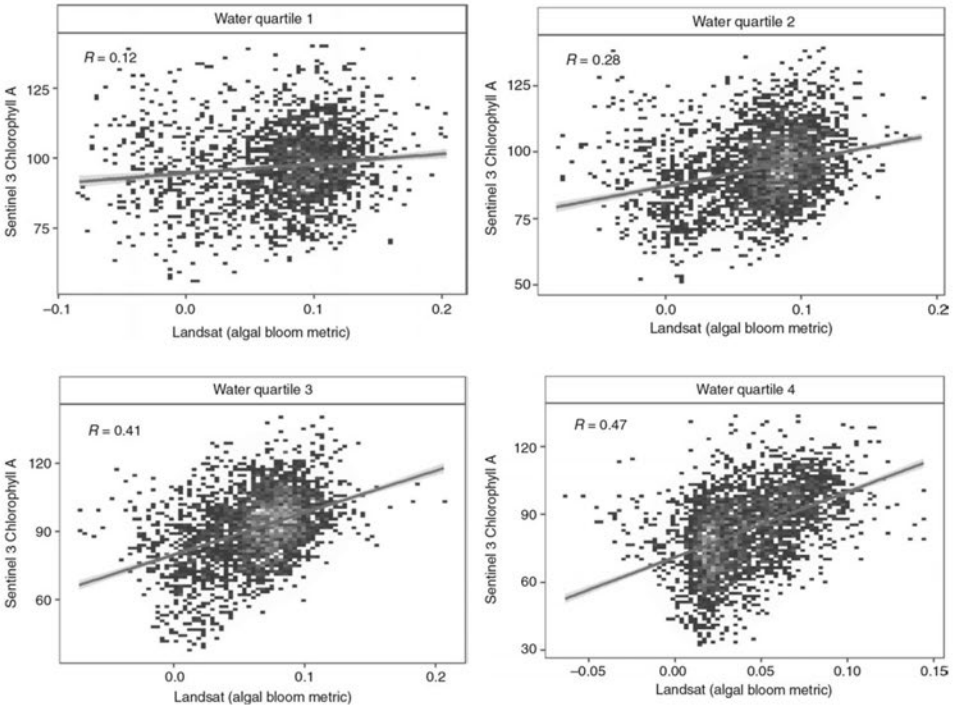

Figure 4A.1 Scatterplot of water quality at the county-year level for Landsat algal bloom measure (x-axis) and Sentinel chlorophyll measure (y-axis) from 2017 to 2020. Outliers outside the 99.9th percentile dropped for clarity. Panels split counties into quartile by water area (1 is least water; 4 is most water). Lighter areas show higher density of points.

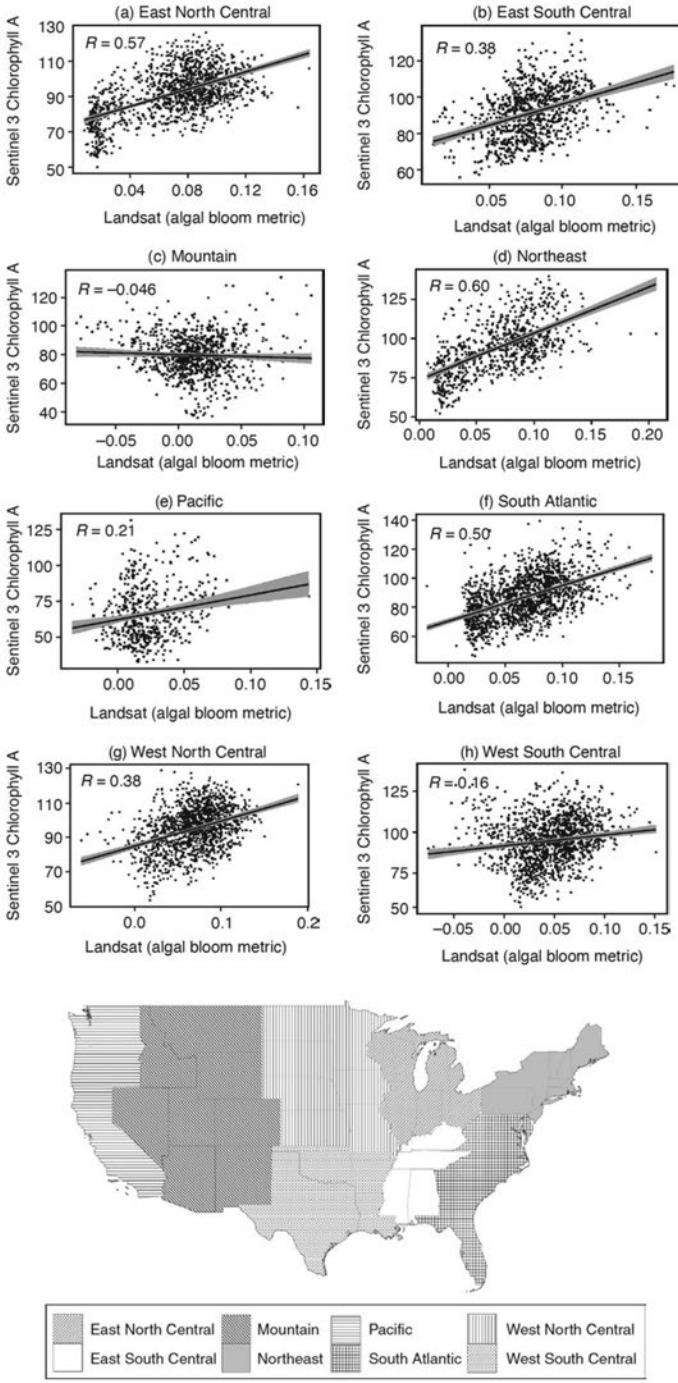

Figure 4A.2 Scatterplot of water quality at the county-year level for Landsat algal bloom measure (x-axis) and Sentinel chlorophyll measure (y-axis) from 2017 to 2020. Outliers outside the 99.9th percentile dropped for clarity, as well as counties with less than 5 km² water area. Panels split counties into US census regions corresponding to the bottom map.

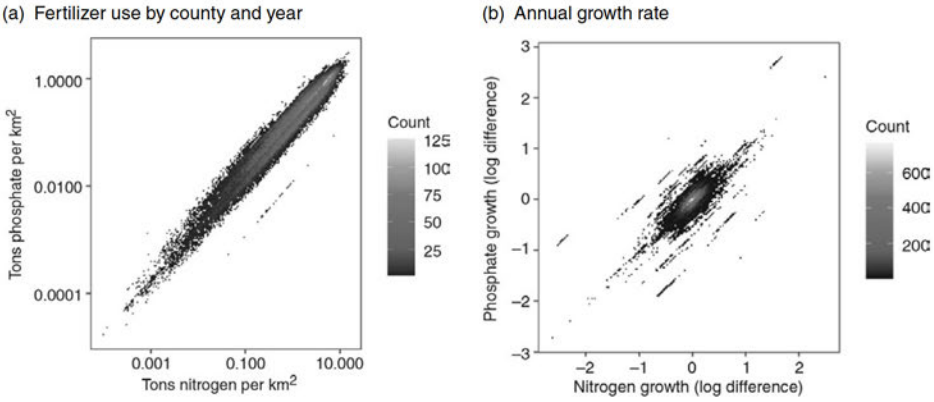

Figure 4A.3 Scatterplot of USGS county-level farm nitrogen and phosphate use per km². Left panel shows annual levels, right panel shows annual change in term of growth rate.

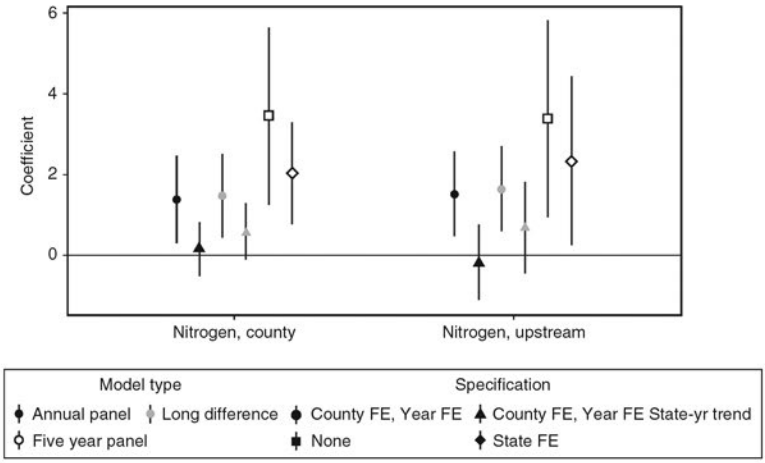

Figure 4A.4 Effect of nitrogen use on late summer algal bloom intensity, no climate controls. Coefficient plot. Same as figure 4.6 except does not include weather controls. Lines with black shapes include the same specification as table 4.4. Lines with gray shapes include observations every five years from 1987 to 2017, using average values in the year prior through the year after each point. Lines with white shapes are the results of the cross-sectional long difference from 1987 to 2017, similarly using three-year average values around the endpoints. All models control for average weather conditions. Counties with less than 5 km² of water dropped from analysis. Standard errors clustered at the state level. Error bars are at the 95 percent confidence range.

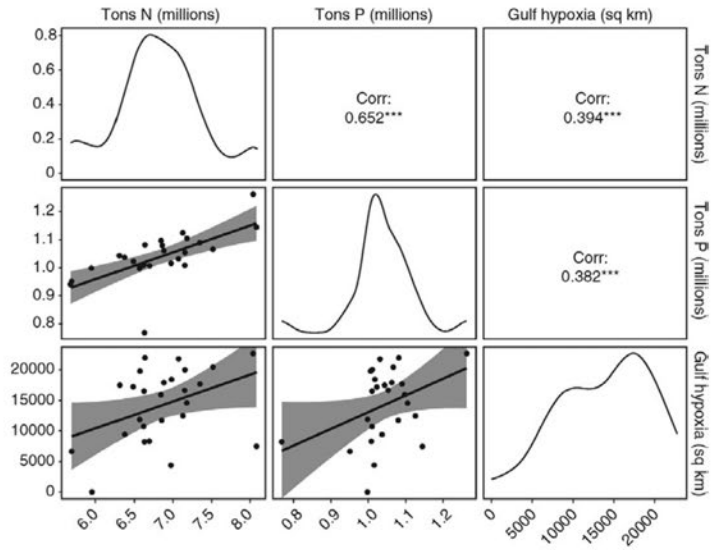

Figure 4A.5 Scatterplots with line of best fit for weighted upstream basin fertilizer use of nitrogen (N) and phosphate (P) in millions of tons and Gulf of Mexico hypoxic zone extent in km². Diagonal line is kernel density plots showing distribution of annual values.

Table 4A.1 Mississippi River basin annual phosphate use and Gulf hypoxia extent

	Dependent variable:					
	Hypoxia (sq km)			Log Hypoxia (sq km)		
	(1)	(2)	(3)	(4)	(5)	(6)
Phosphate	27.314*	26.447**	26.622*			
	(13.499)	(12.068)	(13.379)			
Log Phosphate				3.159	3.207	3.239
				(2.908)	(2.487)	(2.671)
Weather upstream		X	X		X	X
Weather coastal			X			X
Observations	26	26	26	26	26	26
R^2	0.146	0.404	0.404	0.047	0.390	0.415
Adjusted R^2	0.110	0.323	0.255	0.007	0.307	0.269
F Statistic	4.094*	4.975***	2.714**	1.180	4.691**	2.836**

Note: Linear regression. Dependent variable is Gulf of Mexico summer hypoxic extent as defined by the estimated area where bottom-water dissolved oxygen is below 2 mg/L. Phosphate is measured in 1,000s of tons for farm use, inverse weighted by distance from the mouth of the Mississippi River and summed across all counties in the Mississippi River basin. Weather controls include average temperature and precipitation from January to June of the given year for all counties in the Mississippi River basin (upstream) and counties along the coast of the Gulf of Mexico (coastal). Time period from 1985 to 2019. * $p < 0.1$; ** $p < 0.05$; *** $p < 0.01$

References

Anderson, Donald M. 1989. "Toxic Algal Blooms and Red Tides: A Global Perspective." *Red Tides: Biology, Environmental Science and Toxicology*: 11–16.

Barbier, Edward B. 2012. "Progress and Challenges in Valuing Coastal and Marine Ecosystem Services." *Review of Environmental Economics and Policy* 6 (1): 1–19.

Brakebill, J. W., and J. M. Gronberg. 2017. "County-level Estimates of Nitrogen and Phosphorus from Commercial Fertilizer for the Conterminous United States, 1987–2012." US Geological Survey, United States.

Brooks, Bryan W., James M. Lazorchak, Meredith D. A. Howard, Mari-Vaughn V. Johnson, Steve L. Morton, Dawn A. K. Perkins, Euan D. Reavie, Geoffrey I. Scott, Stephanie A. Smith, and Jeffery A. Steevens. 2016. "Are Harmful Algal Blooms Becoming the Greatest Inland Water Quality Threat to Public Health and Aquatic Ecosystems?" *Environmental Toxicology and Chemistry* 35 (1): 6–13.

Buto, Susan G., and Rebecca D. Anderson. 2020. *NHDPlus High Resolution (NHDPlus HR)—A Hydrography Framework for the Nation*. Technical report. US Geological Survey.

Clark, John M., Blake A. Schaeffer, John A. Darling, Erin A. Urquhart, John M. Johnston, Amber R. Ignatius, Mark H. Myer, Keith A. Loftin, P. Jeremy Werdell, and Richard P. Stumpf. 2017. "Satellite Monitoring of Cyanobacterial Harmful Algal Bloom Frequency in Recreational Waters and Drinking Water Sources." *Ecological Indicators* 80: 84–95.

David, Mark B., Laurie E. Drinkwater, and Gregory F. McIsaac. 2010. "Sources of Nitrate Yields in the Mississippi River Basin." *Journal of Environmental Quality* 39 (5): 1657–1667.

Diaz, Robert J., and Rutger Rosenberg. 2008. "Spreading Dead Zones and Consequences for Marine Ecosystems." *Science* 321 (5891): 926–29.

Doney, Scott C. 2010. "The Growing Human Footprint on Coastal and Open-Ocean Biogeochemistry." *Science* 328 (5985): 1512–1516.

Duan, Hongtao, Yuanzhi Zhang, Bai Zhang, Kaishan Song, and Zongming Wang. 2007. "Assessment of Chlorophyll-a Concentration and Trophic State for Lake Chagan Using Landsat TM and Field Spectral Data." *Environmental Monitoring and Assessment* 129 (1–3): 295–308.

Erisman, Jan Willem, James N. Galloway, Sybil Seitzinger, Albert Bleeker, Nancy B. Dise, A. M. Roxana Petrescu, Allison M. Leach, and Wim de Vries. 2013. "Consequences of Human Modification of the Global Nitrogen Cycle." *Philosophical Transactions of the Royal Society B: Biological Sciences* 368 (1621): 20130116.

Falcone, James A. 2021. *Estimates of County-Level Nitrogen and Phosphorus from Fertilizer and Manure from 1950 through 2017 in the Conterminous United States*. Technical report. US Geological Survey.

FAO. 2018. World Fertilizer Trends and Outlook to 2018.

Glibert, Patricia M. 2020. "Harmful Algae at the Complex Nexus of Eutrophication and Climate Change." *Harmful Algae* 91:101583.

Gruber, Nicolas, and James N. Galloway. 2008. "An Earth-System Perspective of the Global Nitrogen Cycle." *Nature* 451 (7176): 293–96.

Hallegraeff, Gustaaf M. 1993. "A Review of Harmful Algal Blooms and Their Apparent Global Increase." *Phycologia* 32 (2): 79–99.

Ho, Jeff C., Anna M. Michalak, and Nima Pahlevan. 2019. "Widespread Global Increase in Intense Lake Phytoplankton Blooms since the 1980s." *Nature* 574 (7780): 667–70.

Ho, Jeff C., Richard P. Stumpf, Thomas B. Bridgeman, and Anna M. Michalak. 2017.

"Using Landsat to Extend the Historical Record of Lacustrine Phytoplankton Blooms: A Lake Erie Case Study." *Remote Sensing of Environment* 191: 273–85.

Hudnell, H. Kenneth. 2008. *Cyanobacterial Harmful Algal Blooms: State of the Science and Research Needs*. Vol. 619. Springer Science & Business Media.

Huisman, Jef, Geoffrey A. Codd, Hans W. Paerl, Bas W. Ibelings, Jolanda M. H. Verspagen, and Petra M. Visser. 2018. "Cyanobacterial Blooms." *Nature Reviews Microbiology* 16 (8): 471–83.

Keiser, David A., and Joseph S. Shapiro. 2019. "Consequences of the Clean Water Act and the Demand for Water Quality." *The Quarterly Journal of Economics* 134 (1): 349–96.

Kling, Catherine L. 2013. "State Level Efforts to Regulate Agricultural Sources of Water Quality Impairment." *Choices* 28 (316–2016–7675).

Metaxoglou, Konstantinos, and Aaron Smith. 2021. "Nutrient Pollution and U.S. Agriculture." Working Paper.

Michalak, Anna M., Eric J. Anderson, Dmitry Beletsky, Steven Boland, Nathan S. Bosch, Thomas B. Bridgeman, Justin D. Chaffin, Kyunghwa Cho, Rem Confesor, Irem Daloglu, et al. 2013. "Record-Setting Algal Bloom in Lake Erie Caused by Agricultural and Meteorological Trends Consistent with Expected Future Conditions." *Proceedings of the National Academy of Sciences* 110 (16): 6448–6452.

Mitsch, William J., John W. Day, Li Zhang, and Robert R. Lane. 2005. "Nitrate-Nitrogen Retention in Wetlands in the Mississippi River Basin." *Ecological Engineering* 24 (4): 267–78.

Monitoring Water Quality, Intergovernmental Task Force on. 1995. *The Strategy for Improving Water-Quality Monitoring in the United States*. USGS Water Information Coordination Program.

Nixon, Scott W. 1995. "Coastal Marine Eutrophication: A Definition, Social Causes, and Future Concerns." *Ophelia* 41 (1): 199–219.

Olmstead, Sheila M. 2010. "The Economics of Water Quality." *Review of Environmental Economics and Policy* 4 (1): 44–62.

Paerl, Hans W., and Jef Huisman. 2008. "Blooms Like It Hot." *Science* 320 (5872): 57–58.

Rabotyagov, Sergey S., Catherine L. Kling, Philip W. Gassman, Nancy N. Rabalais, and Robert Eugene Turner. 2014. "The Economics of Dead Zones: Causes, Impacts, Policy Challenges, and a Model of the Gulf of Mexico Hypoxic Zone." *Review of Environmental Economics and Policy* 8 (1): 58–79.

Read, Emily K., Lindsay Carr, Laura De Cicco, Hilary A. Dugan, Paul C. Hanson, Julia A. Hart, James Kreft, Jordan S. Read, and Luke A. Winslow. 2017. "Water Quality Data for National-Scale Aquatic Research: The Water Quality Portal." *Water Resources Research* 53 (2): 1735–1745.

Ross, Matthew R. V., Simon N. Topp, Alison P. Appling, Xiao Yang, Catherine Kuhn, David Butman, Marc Simard, and Tamlin M. Pavelsky. 2019. "AquaSat: A Data Set to Enable Remote Sensing of Water Quality for Inland Waters." *Water Resources Research* 55 (11): 10012–10025.

Shortle, James, and Richard D. Horan. 2001. "The economics of Nonpoint Pollution Control." *Journal of Economic Surveys* 15 (3): 255–89.

———. 2013. "Policy Instruments for Water Quality Protection." *Annual Review of Resource Economics* 5 (1): 111–38.

Smayda, Theodore J. 1997. "What Is a Bloom? A Commentary." *Limnology and Oceanography* 42 (5, part2): 1132–136.

Steffen, Will, Katherine Richardson, Johan Rockström, Sarah E. Cornell, Ingo Fetzer, Elena M. Bennett, Reinette Biggs, Stephen R. Carpenter, Wim De Vries,

Cynthia A. De Wit, et al. 2015. "Planetary Boundaries: Guiding Human Development on a Changing Planet." *Science* 347 (6223).

Taylor, Charles A., and Hannah Druckenmiller. 2021. "Wetlands, Flooding, and the Clean Water Act." Working Paper.

Tebbs, E. J., J. J. Remedios, and D. M. Harper. 2013. "Remote Sensing of Chlorophyll-A as a Measure of Cyanobacterial Biomass in Lake Bogoria, A Hypertrophic, Saline–Alkaline, Flamingo Lake, Using Landsat ETM+." *Remote Sensing of Environment* 135: 92–106.

Topp, Simon N., Tamlin M. Pavelsky, Emily H. Stanley, Xiao Yang, Claire G. Griffin, and Matthew R. V. Ross. 2021. "Multi-decadal Improvement in US Lake Water Clarity." *Environmental Research Letters* 16 (5): 055025.

Turner, R. Eugene, and Nancy N. Rabalais. 2013. "Nitrogen and Phosphorus Phytoplankton Growth Limitation in the Northern Gulf of Mexico." *Aquatic Microbial Ecology* 68 (2): 159–69.

Tyler, A. N., E. Svab, T. Preston, M. Présing, and W. A. Kovács. 2006. "Remote Sensing of the Water Quality of Shallow Lakes: A Mixture Modelling Approach to Quantifying Phytoplankton in Water Characterized by High-Suspended Sediment." *International Journal of Remote Sensing* 27 (8): 1521–1537.

Vitousek, Peter M., John D. Aber, Robert W. Howarth, Gene E. Likens, Pamela A. Matson, David W. Schindler, William H. Schlesinger, and David G. Tilman. 1997. "Human Alteration of the Global Nitrogen Cycle: Sources and Consequences." *Ecological Applications* 7 (3): 737–50.

Wang, Menghua, and Wei Shi. 2007. "The NIR-SWIR Combined Atmospheric Correction Approach for MODIS Ocean Color Data Processing." *Optics Express* 15 (24): 15722–15733.